BIOINFORMATICS

Vol. 21 Suppl. 1 2005, pages i232–i240
doi:10.1093/bioinformatics/bti1036

Modeling the organization of the WUSCHEL *expression domain in the shoot apical meristem*

Henrik Jönsson[1], Marcus Heisler[2,†], G. Venugopala Reddy[2,†], Vikas Agrawal[2], Victoria Gor[3], Bruce E. Shapiro[3], Eric Mjolsness[4,5,] and Elliot M. Meyerowitz[2]*

[1]Department of Theoretical Physics, Complex Systems Division, Lund University, Sweden, [2]Division of Biology and [3]Jet Propulsion Laboratory, California Institute of Technology, CA, USA,and [4]School of Information and Computer Science and [5]Institute for Genomics and Bioinformatics, University of California, Irvine, CA, USA

Received on January 15, 2005; accepted on March 27, 2005

ABSTRACT

Motivation: The above-ground tissues of higher plants are generated from a small region of cells situated at the plant apex called the shoot apical meristem. An important genetic control circuit modulating the size of the *Arabidopsis thaliana* meristem is a feed-back network between the *CLAVATA3* and *WUSCHEL* genes. Although the expression patterns for these genes do not overlap, WUSCHEL activity is both necessary and sufficient (when expressed ectopically) for the induction of *CLAVATA3* expression. However, upregulation of *CLAVATA3* in conjunction with the receptor kinase CLAVATA1 results in the downregulation of *WUSCHEL*. Despite much work, experimental data for this network are incomplete and additional hypotheses are needed to explain the spatial locations and dynamics of these expression domains. Predictive mathematical models describing the system should provide a useful tool for investigating and discriminating among possible hypotheses, by determining which hypotheses best explain observed gene expression dynamics.

Results: We are developing a method using *in vivo* live confocal microscopy to capture quantitative gene expression data and create templates for computational models. We present two models accounting for the organization of the *WUSCHEL* expression domain. Our preferred model uses a reaction-diffusion mechanism in which an activator induces *WUSCHEL* expression. This model is able to organize the *WUSCHEL* expression domain. In addition, the model predicts the dynamical reorganization seen in experiments where cells, including the *WUSCHEL* domain, are ablated, and it also predicts the spatial expansion of the *WUSCHEL* domain resulting from removal of the CLAVATA3 signal.

Availability: An extended description of the model framework and image processing algorithms can be found at http://www.computableplant.org, together with additional results and simulation movies.

Contact: emj@uci.edu

Supplementary information: http://www.computableplant.org/ and alternatively for a direct link to the page, http://computableplant.ics.uci.edu/bti1036 can be accessed.

1 INTRODUCTION

Developmental biological systems consist of intracellular molecular regulation networks combined with intercellular signals and transport, resulting in complex interaction networks with the ability to control the development of multicellular organisms. Experimental data of important molecular agents and interactions are most often incomplete, and additional hypotheses are needed to explain their spatial and dynamical behavior.

Mathematical modeling provides a powerful method for describing and testing hypotheses about developmental biological systems. Not only can hypotheses be tested to see whether they account for the observed data but also predictions can be made for new experiments. So far, computational models for developmental multicellular systems have mostly been developed for *Drosophila* [see e.g. von Dassow *et al*. (2000); Mjolsness (2001); Jaeger *et al*. (2004)], but there are also examples for modeling plant development [see for a review Prusinkiewicz (2004)].

The shoot apical meristem (SAM) plays a central role in the development of the aerial part of a plant (Steeves and Sussex, 1998; Meyerowitz, 1997; Weigel and Jurgens, 2002). Throughout the life of a plant, it provides new cells to the stem, and it is also the site for the formation of new leaf and flower primordia. Within the SAM, spatial regions of cells are characterized by different gene expression patterns. Although cells continue to proliferate, and individual cells move in and out of these regions, the spatial domains stay constant. This indicates that the organization of the SAM is controlled by intrinsic intercellular signaling, more than by

*To whom correspondence should be addressed.

†These authors contributed equally to this work.

inheritance of information along cell lineage. This signaling network must be highly robust, since the actual shape and size of the SAM vary somewhat during the growth of the plant, and considerably among individual plants.

More evidence of the robustness of the network controlling development can be seen in different physical perturbation experiments. Dissection of the SAM, and even fine-tuned cell ablation experiments, show that spatial expression patterns 'self-organize' into their normal patterns, with continued shoot growth as a result (or even the organization of more than one continued shoot) (Reinhardt *et al*., 2003).

Essential for the control of SAM development in *Arabidopsis thaliana* is a feed-back network between the genes *CLAVATA3 (CLV3)* and *WUSCHEL (WUS)* (Sharma *et al*., 2003; Weigel and Jurgens, 2002). The expression domains of these genes are not spatially overlapping, and intercellular signaling is essential for their mutual regulation to function. In a series of publications (Fletcher *et al*., 1999; Brand *et al*., 2000; Schoof *et al*., 2000), these regulatory interactions have been elucidated mainly through the study of loss-of- function and gain-of-function experiments. The current conclusion is that *WUS* induces *CLV3*, and that the intercellular CLV3 acts as a ligand that, together with the receptor kinase CLAVATA1 (CLV1), activates a signal that represses *WUS* (Sharma *et al*., 2003).

In this work, we address the question of how the *WUS* expression pattern is activated and confined to a small region of cells located centrally in the SAM. We do this by combining *in vivo* confocal microscopy data with computer simulations of different models for *WUS* activation. An important step in the methodology is the attempt to quantitatively measure *WUS* expression. Using a set of image processing tools, we compartmentalize and quantify the confocal microscopy data, resulting in an approximate cell-based quantitative template for *WUS* expression.

A complete model for SAM development would need to include biochemical reactions, intercellular molecular transportation and signaling, cellular growth and proliferation as well as mechanical interactions. We are developing tools for dealing with all apects of SAM development with the goal of combining them into a single model. For now, we disregard cellular growth and proliferation (therefore making mechanical interactions irrelevant). The system is further simplified to a two-dimensional description of the problem, where CLV3 is not explicity modeled, but is rather included as a repressing signal. We use cell-based compartments and model molecular reactions and regulations using basic biochemical rules, and molecular transport is modeled as diffusion. A continuous deterministic approach is used to model the dynamics, using ordinary differential equations.

The concept of pattern-forming reaction-diffusion models within biology was first introduced by Turing (1952), and since then multiple variants have been used to explain various patterns in nature (Meinhardt, 1982). The dynamics of these models is such that they can form patterns with high regularity from a close-to-homogeneous concentration distribution. Typically concentration peaks form with a regular distance between the peaks, and this distance is dependent on the model parameters. We note the similarity of a spontaneous peak forming in such models to the centrally located and spatially restricted activation of *WUSCHEL*, and we will use such a model for inducing *WUS*. We have chosen to use the Brusselator model (Prigogine and Lefever, 1968), although we could have chosen any pattern-forming reaction-diffusion model.

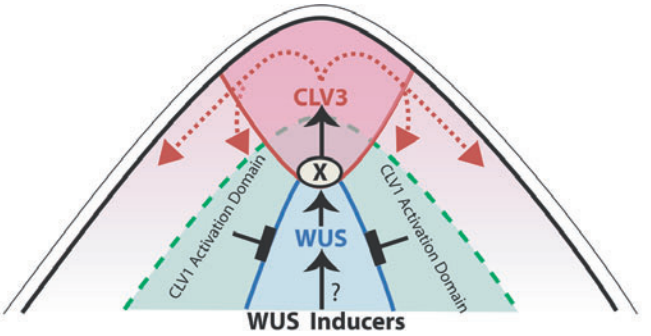

Fig. 1. A schematic of the expression domains of *CLAVATA1*, *CLAVATA3* and *WUSCHEL*. The solid arrows indicate the regulatory (indirect) interactions and the dashed arrows show the movement of the CLV3 protein.

2 SYSTEM AND METHODS

2.1 Organization of the shoot apical meristem

Throughout the life of a plant, the SAM includes a region of cells expressing *CLAVATA3* which are often regarded as the plant stem cells (Weigel and Jurgens, 2002). The *CLV3* gene is expressed at the very apex in a cone shaped region (Fig. 1) (Fletcher *et al*., 1999), and the CLV3 protein is secreted and moves laterally from the region in which it is transcribed (dashed arrows in Fig. 1) (Lenhard and Laux, 2003). A couple of cells below the apex, a small region of cells expresses the homeodomain transcription factor WUSCHEL (Fig. 1) (Mayer *et al*., 1998). This region is often referred to as the organizing center, and here, in a somewhat larger region compared with WUS, the gene encoding for the receptor kinase CLAVATA1 is also expressed (Fig. 1) (Clark *et al*., 1997).

In a series of loss-of-function and gain-of-function experiments, the interactions between the *WUSCHEL* and *CLAVATA* genes have been characterized (Fletcher *et al*., 1999; Brand *et al*., 2000; Schoof *et al*., 2000). The conclusions from these experiments are that *WUS* induces both *CLV* genes, and that CLV3 acts as a ligand for the CLV1 receptor kinase which, upon binding, activates a signal repressing *WUS*.

Although there is a large amount of data supporting this scenario, there are still many open questions regarding this network. One is the spatial asymmetry of the domains: if *WUS*

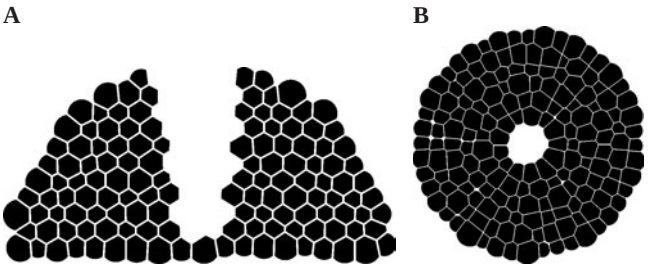

Fig. 2. A schematic figure of the cells removed in the laser ablation experiment (Reinhardt *et al*., 2003). The central zone with the *CLV3* expressing cells and the organizing center and its *WUS* expressing cells are ablated. (**A**) Vertical section through the center of the SAM. (**B**) Horizontal section through the organizing center.

induces *CLV3* expression, why is *CLV3* expressed only in a region above the *WUS* domain? This question was addressed in a model by Jönsson *et al*. (2003) where the WUS signal was combined with a signal originating from the outer layer of cells (the L1 layer) to induce *CLV3* expression. The model was able to correctly mimic the *CLV3* expression domain, given the location of the *WUS* expression domain. Another open question is how the *WUS* expression pattern is controlled, and this is the main question addressed in this paper.

2.1.1 WUSCHEL *expression and dynamics* In the adult plant, *WUS* is expressed in the organizing center in both vegatitive and inflorescence SAMs (Fig. 1) (Mayer *et al*., 1998). *WUS* expression is also turned on in floral meristems during early stages of flower development.

In *clv* loss of function mutants, the size of the *WUS* expression domain is increased (in these mutants, the SAM itself is enlarged, and enlarged *CLV* expression domains are also seen) (Fletcher *et al*., 1999). It should be noted that, although the *WUS* domain is increased in size, spatial restriction on the expression region can still be observed.

Models describing SAM dynamics need to account for the ability of the expression domains to self-organize and reorganize. Reinhardt *et al*. (2003) recently performed an experiment in which subsets of cells in the tomato SAM were ablated, creating a hole in the center of the SAM and removing the cells of the organizing center (Fig. 2). The dynamics of *WUS* expression was then followed during SAM reorganization. After the ablation, new *WUS* expression first reappeared at low levels in a ring-shaped domain surrounding the ablated area. At a later time point either one or two smaller, strongly expressing domains appeared, and for each domain a normal growing shoot developed. In this case the two new domains were situated on opposite sides of the ablated region.

2.2 Confocal microscopy

We have recently developed an *in vivo* live imaging technique which allows periodic imaging of the SAM over several days (Reddy *et al*., 2004). The method utilizes confocal microscopy, in conjunction with either dyes or green fluorescent protein (GFP) constructs that are used for labeling cell structures or important proteins. Here, we will use a SAM doubly labeled with a cell membrane dye marker (FM4-64) and a construct where the WUS promoter drives green fluorescent protein (*pWUS*::GFP, Fig. 3). From this we extract a template which is used for comparison with the models. The technique enables the recording of expression patterns in three dimensions over time, but here we use data from a single section corresponding to a single time point to represent the equilibrium state in a non-growing simulation.

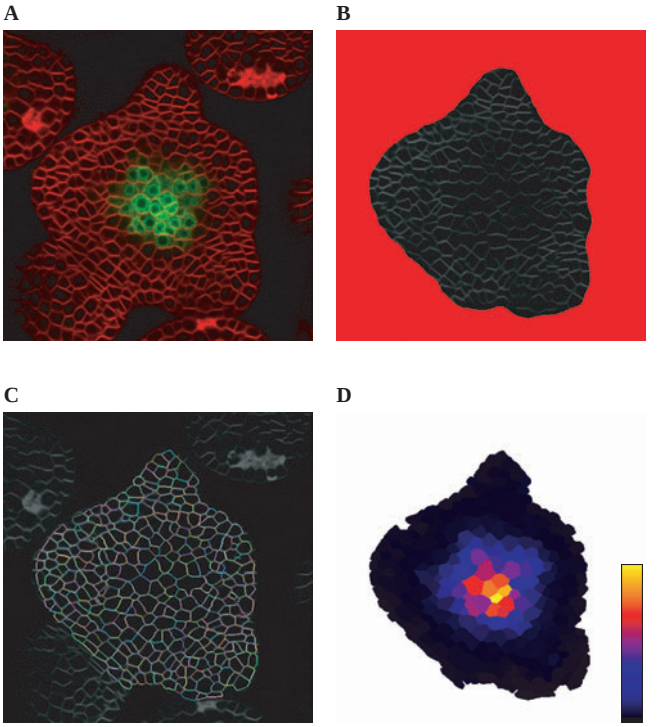

Fig. 3. Quantification of the *WUS* expression. (**A**) A doubly labeled confocal image showing a horizontal section ∼17 μm into the plant shoot. A cell membrane dye marker is shown in red, and fluorescence resulting from expression of a where the WUS promoter drivers green fluorescent protein a *pWUS*::GFP construct is shown in green. (**B**) Pixels extracted as background. As can be seen, older primordia are not included in the SAM template. (**C**) Walls (defined by the borders between cell compartments) extracted by the watershed algorithm. (**D**) Average *pWUS*::GFP intensity for individual cells. These numbers are interpreted as relative concentrations. The color coding is defined as black (min)–blue–red–yellow (max).

2.3 Image processing

To be able to compare models with the data provided by the confocal imaging technique, quantification of the image data is essential. We use different image processing algorithms to extract cell compartments and GFP fluorescence intensities within individual cells. For simplicity, we assume that the GFP intensity is linearly related to the amount of protein, and

hence interpret the average intensity within a cell as a relative protein concentration. More detailed information about the algorithms used is provided as Supplementary information, but, in short, the methodology and algorithms used are the following:

(1) *Background extraction*. In the present study, a snake algorithm working on a gradient vector flow field is used to extract the background in the membrane picture (Xu and Prince, 1998). It is manually initiated by clicking around the SAM, after which the edge of the SAM is located in the picture (Fig. 3B).

(2) *Cell extraction*. Cells are extracted from the membrane picture using a watershed algorithm (Gonzalez and Woods, 2002). The algorithm starts in each pixel and walks downhill in the 'intensity landscape' until it reaches a minimum. All pixels that end up in a single minimum are regarded as one cell. A picture of the borders of the extracted cells can be seen in Figure 3C. A beneficial feature of this algorithm is that it is easy to extract neighborhood relationships, including the length of the 'wall' connecting two neighbors. Included in this algorithm is a preprocessor that reduces noise by a simple region averaging.

(3) *Gene expression extraction*. By using the cell information extracted from the membrane picture, the average intensity within each pixel subset defining a cell is extracted from the *pWUS*::GFP picture (Fig. 3D).

2.4 Modeling

A complete model for developmental biological systems needs to account for a diverse set of biological, chemical and physical features. Included among these are molecular reactions, gene regulation, intercellular molecular transport and signaling, cell growth and proliferation, and mechanical interactions between cells. The models presented in this work describe only a subset of these features, which will be discussed in more detail below.

We use spatial compartmentalization at a cellular level and do not account for cellular growth or proliferation. Molecular levels are described by concentrations, and deterministic ordinary differential equations (ODEs) are used for describing the dynamics. The models presented here are built from three main components:

(1) *Molecular reactions*. Basic mass action kinetics is used, where reaction rates are proportional to the concentration of reactants.

(2) *Gene regulation*. We use sigmoidal functions to describe the interactions in a gene regulatory network (GRN) (Mjolsness *et al*., 1991; Mjolsness, 2001). The regulation of a gene i, modeled as the change in the corresponding protein concentration v_i, is defined by

$$\frac{\mathrm{d}v_i}{\mathrm{d}t} = \frac{1}{\tau_i} g\left(\sum_j T_{ij} v_j + h_i\right), \tag{1}$$

where $g(x)$ is the sigmoidal function

$$g(x) = \frac{1}{2}\left(1 + \frac{x}{\sqrt{1+x^2}}\right). \tag{2}$$

The parameter τ_i is the inverse maximal rate, and h_i sets the basal expression level. The T_{ij} parameters define the strength of the regulation (j regulating i). A positive T defines an activation, whereas a negative T leads to a repression.

(3) *Molecular transport*. Transport between neighboring cells is modeled by a passive diffusion. The transport of a molecule x between two cells i, j is, in our ODE setting, modeled as

$$\frac{\mathrm{d}x_i}{\mathrm{d}t} = D(x_j - x_i), \tag{3}$$

where D is the diffusion constant. When simulating on a template where more spatial properties are accounted for, the more detailed model is

$$\frac{\mathrm{d}x_i}{\mathrm{d}t} = D' \frac{A_{ij}}{d_{ij} V_i}(x_j - x_i), \tag{4}$$

where A_{ij} is the intersection area between the cells and d_{ij} is the distance between the cell centers. V_i is the cell volume and accounts for the fact that the number of molecules leaving one cell is the same as the number that enter the next. The diffusion constants are related to the lattice constants by $D' = k_D D$ to compensate for the spatial contributions introduced.

2.4.1 Basic assumptions of the models The main question addressed in this paper is how the sharply restricted *WUSCHEL* expression pattern forms at the center of the SAM (Figs 1 and 3). Both models presented here utilize a repressive signal originating from the surface cells (L1 layer). We have previously shown how such a signal may be dynamically maintained (Jönsson *et al*., 2003). As discussed in section 2.1, part of this signal might originate from CLV3 moving laterally from its expression domain (Fig. 1). The repressive signal is combined with *WUS* activation, for which two different hypotheses are compared in this study.

We restrict simulations to two-dimensional sections of the SAM. This sets some limitations on how well the models can predict experimental data, as will be discussed in the Results and Discussion section. The main results, on the other hand, are not dependent on this. Essentially, only an additional repression in/from the stem is needed for the models to be extended into three dimensions.

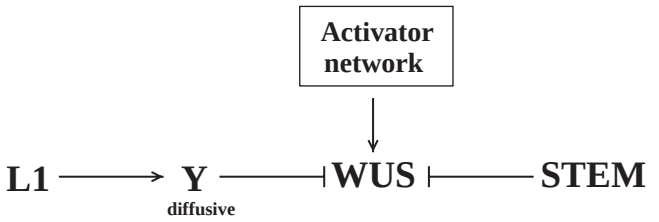

Fig. 4. A schematic illustration of the activator model. The activator network produces a pattern of an activator molecule which is inducing *WUS*. This activation is combined with a repressing signal originating from the surface layer of cells. The repressive contribution originating from the stem is not applicable in our two-dimensional system, but is needed in a three-dimensional model.

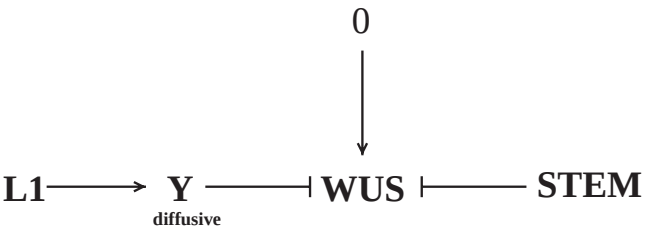

Fig. 5. A schematic illustration of the repressor model. The *WUS* expression is normally on ($0 \rightarrow WUS$) in all cells. The *WUS* expression domain is restricted by the repressive signal described in Figure 4.

Table 1. Parameter values used in the simulations

Parameter	Activator model	Repressor model
k_y, d_y, D_y, k_D	0.2, 0.1, 0.1, 3.0	0.2, 0.1, 0.1, 3.0
τ_w, d_w, h_w, T_{wy}	10, 0.1, 0, −20	10, 0.1, 2, −30
T_{wa}	0.5	
a, b, β, c	0.1, 0.2, 0.1, 0.1	
d, D_a, D_b	0.01, 0.1, 1.5	

2.4.2 Activator model The main assumption in this model is that *WUS* expression is induced by an activator produced by a pattern-forming, reaction-diffusion model (Fig. 4) (Meinhardt, 1982). Inherent in the activator model dynamics is the ability to create regular patterns of activator concentrations at distinct spatial distances, even from close-to-homogeneous initial concentrations. The distances between concentration peaks can be tuned by model parameters to allow for only a single peak within the SAM. To ensure that the activator peak is positioned at the center of the SAM, a small repression of the activator from an L1 originating signal is included.

The only intercellular interaction within the model is the passive transport of diffusive molecules (denoted using the ∇^2 operator in the equations). The model is defined as

$$\frac{\mathrm{d}W}{\mathrm{d}t} = \frac{1}{\tau_w} g\left(h_w + T_{wa}A + T_{wy}Y\right) - d_w W, \quad (5)$$

$$\frac{\mathrm{d}Y}{\mathrm{d}t} = k_y L_1 - d_y Y + D_y \nabla^2 Y, \quad (6)$$

$$\frac{\mathrm{d}A}{\mathrm{d}t} = a - (b+\beta)A + cA^2B - dY + D_a \nabla^2 A, \quad (7)$$

$$\frac{\mathrm{d}B}{\mathrm{d}t} = bA - cA^2B + D_b \nabla^2 B. \quad (8)$$

W is the WUS concentration. It is induced by the activator A, repressed by Y, and also has a simple degradation term. Y is the diffusive L1 originating signal molecule, which is constantly induced by L_1, and also has a simple degradation. L_1 is treated as a boundary condition, and is present only in the outermost layer of cells (L1 layer); hence we model the production of Y using a linear term (which becomes boolean in this setup). Among the different available activator models, we have chosen to use the Brusselator model, which is considered simple yet robust in its pattern-forming abilities (Prigogine and Lefever, 1968). We will not go into details about the Brusselator model since it is outside the scope of this work, but note only that Equations (7) and (8) are the standard equations except for the $-dY$ term in Equation (7), which is the included repression from Y, modeled as an increased activator degradation.

2.4.3 Repressor model We have also implemented a model with a simpler hypothesis for the activation of *WUS* expression (Fig. 5). The basic idea of this model is that *WUS* is normally expressed everywhere, unless a repressor is present. In the model, an L1 originating signal represses *WUS* expression, and the ODE equations are defined by

$$\frac{\mathrm{d}W}{\mathrm{d}t} = \frac{1}{\tau_w} g\left(h_w + T_{wy}Y\right) - d_w W, \quad (9)$$

$$\frac{\mathrm{d}Y}{\mathrm{d}t} = k_y L_1 - d_y Y + D_y \nabla^2 Y. \quad (10)$$

W is again the WUS concentration, and it is repressed by the L1 originating signal Y. A term $h_w > 0$ is used to define a basal expression level for *WUS*. It also has a simple degradation term. The equation for Y is exactly the same as in the activator model, and again L_1 is treated as a boundary condition (present only in the L1 layer).

2.4.4 Parameters and initial values The main point in this paper is to show the behavior of different conceptual models for *WUS* activation. A complete investigation of the parameter space, or an optimization of the parameter values, has not been carried out. Instead, we have coarsely adjusted the parameters to approximately fit the data, and we have tried to use the same parameter values for both models where applicable. For completeness, we present the values for all parameters used in the simulations in Table 1.

In the template simulations a more detailed model for diffusion is used [Equation (4)] in which the topological properties are accounted for. The extracted space is 'normalized' to get an average cell volume equal to one. Note that we use exactly the same parameter values for both models when simulated on the template as is used for the lattice simulations, except for the compensation in diffusion constants ($D' = k_D D$) owing to the spatial contributions. This indicates a robustness for both the models.

We start the simulations in a state where the W and Y concentrations are zero in all cells. L_1 is set to one in the surface (L1 layer) cells and zero in all other cells. L_1 is not updated, and this arrangement sets production of Y only in the L1 layer cells. The Brusselator molecules, A and B, are initiated to a small random value ($[0 : 0.1]$) in each cell to avoid a completely homogeneous state. This randomness does not influence the equilibrium state of the system or any of the results.

3 IMPLEMENTATION

The software used for this work was developed by the authors and implemented mostly in C++. The exception is the snake algorithm for extracting background pixels, which is implemented in Matlab and uses the GVF package (http://iacl.ece.jhu.edu/projects/gvf/).

The model simulator is implemented in C++ and designed for multicellular modeling. In addition to what is described in this paper, it also allows for cell–cell signaling, cell growth and proliferation, and mechanical interactions between cells (Jönsson *et al*., 2004; Jönsson and Levchenko, 2005). In all simulations presented in this work, a fifth-order Runge–Kutta solver with adaptive stepsize is used for the numerical integration of the ODEs (Press *et al*., 1992).

Visualizations have been made using C++ software that reads the simulator output and creates tiff (template simulations) or postscript (lattice simulations) output.

4 RESULTS AND DISCUSSION

4.1 Simulations on a template, wild-type behavior

We first set out to determine how well the models recreate the wild-type *WUSCHEL* expression domain. We chose to perform these simulations on the extracted template in order to directly compare the result with the quantified experimental data (Fig. 3). The equilibrium WUS concentration is presented in Figure 6. As can be seen in the figure, the equilibrium expression for both models defines a small, fairly distinct region of *WUS* expression in the central part of the meristem, similar to the experimental data. The spatial position of the *WUS* expression domains in the two models are slightly different from the experimental position (cf. Figs 3 and 6). The positioning in the models depends on the L1 originating signal Y, which in turn depends on the topology of the L1 layer. In Figure 6C and D, the equilibrium concentrations for Y and L_1 (which is marking the L1 layer) are presented. The shift in position might be a consequence of implementing the models in two dimensions, since the actual peak position is determined by the complete three-dimensional contribution of the repressing signal. In Figure 6 the equilibrium concentrations for A and B are also presented. The activator A is a smoother version of WUS levels, and B is almost the inverse of A. When looking at the activator concentration, it is obvious that the L1 originated signal Y is not necessary in the activator model to create a spatially distinct *WUS* expression domain, but Y is included based on the experimental data.

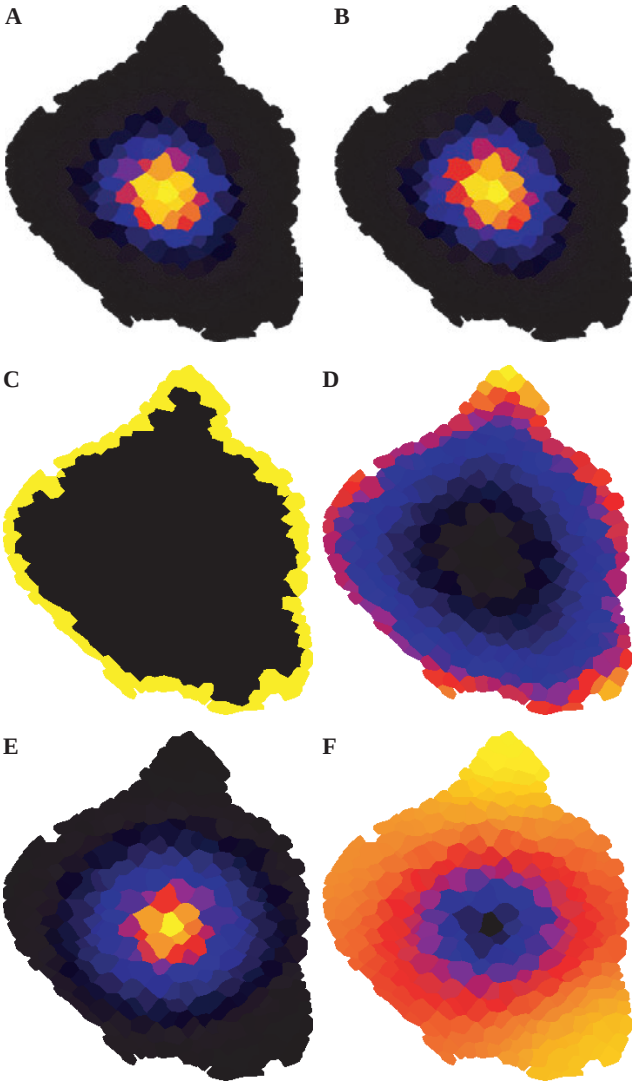

Fig. 6. Equilibrium concentration for different molecules for both models simulated on the extracted template. (**A**) WUS in the activator model. (**B**) WUS in the repressor model. (**C**) L_1 in both models (which is not updated during the simulations). (**D**) Y in both models. (**E**) The activator A (only present in the activator model). (**F**) The inhibitor B (only present in the activator model). Color coding as in Figure 3.

Note also that, although the simulations were carried out on a non-growing template, the models are not sensitive to individual cell positions, and as long as the L1 layer of cells stays intact the models will also be applicable to growing plants.

4.2 Lattice simulations

In the previous section we studied the equilibrium expression of *WUS*. In this section we will study two perturbation experiments discussed in Section 2.1.1. We do this in a lattice setting, and we note that the equilibrium expression patterns are satisfactory since both models create WUS peaks in the central region of the SAM (Fig. 7A and B).

4.2.1 Decreasing the repressing signal As a first perturbation to the system, we look at the dynamics resulting from a weakened repressive signal. This can be interpreted as a weakening or removal of CLV3. As discussed in Section 2.1.1, it is expected that the *WUS* region will expand. The equilibrium concentrations of WUS for both models are presented in Figure 7B and C. In both models, the *WUS* expression domain increases in size, with the behavior more exaggerated in the repressor model. The activator model can hence be interpreted as being more robust to fluctuations of the repressing signal. Robustness is in general a favorable feature of a model, especially in this case, considering that these expression domains are stable over time and are very similar in different plants. However, we do not draw any conclusions from this since the robustness should, rather, be investigated for the complete feed-back network, which is out of the scope of these models.

4.2.2 Laser ablation experiment An important feature of the SAM, including the *WUS* expression domain, is the capability of reorganization, which we address by modeling the laser ablation experiment described in Section 2.1.1. To do this, the central cells are removed from the SAM, and the models are simulated on the new lattice (Fig. 7E–G). In the laser ablation simulation, the activator model creates two new, spatially distinct *WUS* domains at opposite sides of the ablated region. This is in full agreement with the experiment [c.f. Section 2.1.1 and Reinhardt *et al*. (2003)]. Furthermore, this simulation recreates the dynamics of the experiment, since it first induces a circular domain of weakly expressing *WUS* cells surrounding the ablated cells.

The repressor model, on the other hand, does not induce any spatially distinct *WUS* domain. The equilibrium *WUS* expression is in a ring-shaped domain surrounding the ablated cells with fairly low expression.

Hence, the activator model exhibits the very important ability to recreate a spatially distinct *WUS* expression domain from a physically perturbed system. Since this is a feature of the actual biological mechanism, it is a required property for any model trying to address the mechanism underlying *WUS* expression.

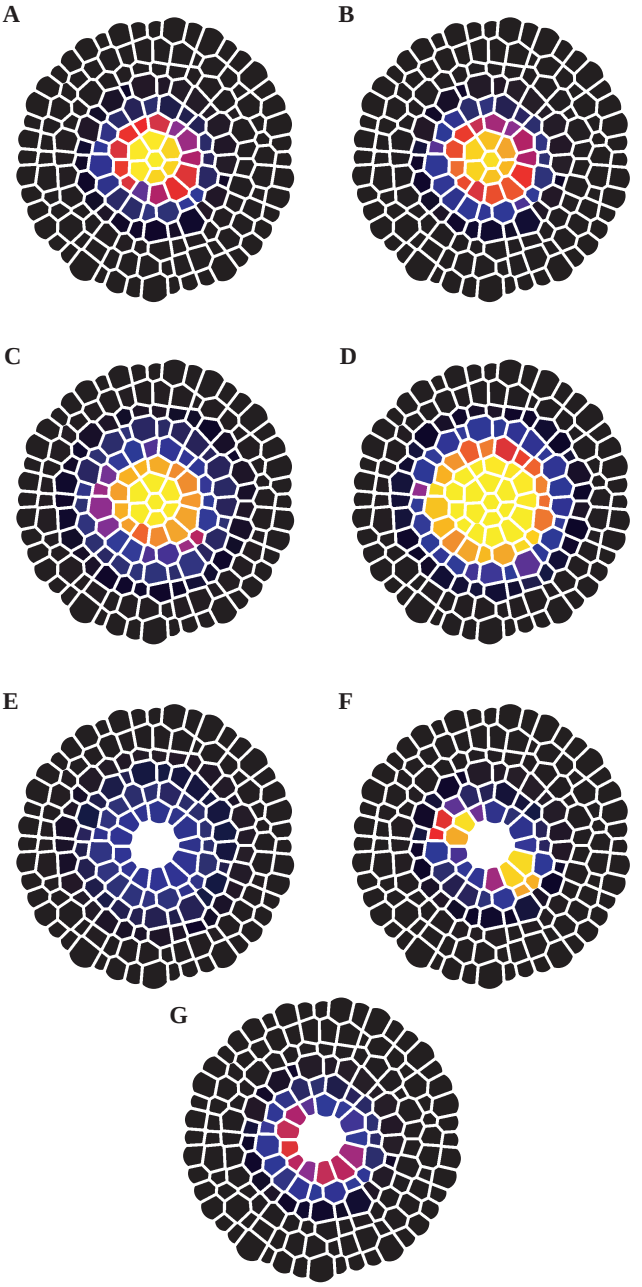

Fig. 7. WUS protein concentrations in lattice simulation. (**A**)–(**B**) Equilibrium concentrations in simulations of the unperturbed model. (**A**) Activator model. (**B**) Repressor model. (**C**)–(**D**) Simulations of a perturbed system where the repressive signal is reduced by a factor of two. The parameter k_y is set to half its original value. (**C**) Activator model. (**D**) Repressor model. (**E**)–(**G**) Simulations of the laser ablation experiment. (**E**) Early time point for the activator model. (**F**) Equilibrium concentration for the activator model. (**G**) Equilibrium concentration for the repressor model. Color coding as in Figure 3. In (**C**)–(**G**), the maximal color value is set to the maximal value in the unperturbed situation ((**A**), (**B**)).

5 CONCLUSION

We have presented a methodology in which *in vivo* confocal microscopy data for the SAM are quantified and used as a template for *in silico* simulations of multicellular models of molecular interaction networks in the SAM. The methodology was demonstrated for a two-dimensional section of the SAM, and for one time point only. We are currently developing the methods to be applicable to time-lapse data for three-dimensional confocal datasets. Typically, the confocal microscope technique enables the collection of fluorescence data for a small number of GFP spectral variants over a period of a couple of days. It is not a high-throughput technique, but the sub-cellular resolution *in vivo* is highly valuable when trying to resolve the dynamics of important proteins. The time frame is also sufficient since the plastochron rate (time between the formation of consecutive leafs/flowers) is of the order of 24 h in *Arabidopsis*.

The main significance of this work is the introduction of a novel model that accounts for both the dynamics and the spatially distinct location of the *WUSCHEL* expression domain within the SAM. *WUS* is a highly significant gene controlling the development of the SAM, and the mechanisms that control its spatial expression pattern are, to a large extent, still unknown. The main conceptual hypothesis of our model is that the dynamics are controlled by a pattern-forming reaction-diffusion mechanism. This mechanism is able to create concentration peaks of an activator molecule at distinct spatial distances from each other. Correctly tuned, it creates only one peak within the SAM, and a small repressive signal from the L1 layer of cells (and from the stem) suffices to place the peak at the correct position of the organizing center. The activator is used to induce *WUS* expression and it regulates the *WUS* expression together with a repressive signal originating from the L1 layer of cells. The repressive signal can be interpreted as the CLV3 signal.

A key feature of the model, apart from its ability to mimic the wild-type *WUS* expression domain, is its ability to reorganize into distinct patterns in a physically perturbed SAM. This was demonstrated by simulation of an experiment in which the cells of the organizing center were ablated.

Finally, the model may also account for the formation of distinct *WUSCHEL* expression regions within newly formed flower meristems. This could follow from the relatively large distance between flower primordia and inflorescence meristem or, alternatively, the flower boundary region may act as a barrier to the meristem-produced inhibitor.

Live imaging using confocal microscopy and the techniques of computational modeling together provide a powerful set of tools to dissect in new ways the complex interaction networks underlying the development and maintenance of the plant SAM.

ACKNOWLEDGEMENTS

We are grateful to Ylva Aspenberg for implementing the image background-extraction algorithm. This research was supported by NSF:FIBR award number EF-0330786. H.J. was supported in part by the Knut and Alice Wallenberg Foundation through Swegene.

REFERENCES

Brand,U., Fletcher,J.C., Hobe,M., Meyerowitz,E.M. and Simon,R. (2000) Dependence of stem cell fate in *A*rabidopsis on a feedback loop regulated by CLV3 activity. *Science*, **289**, 617–619.

Clark,S.E., Williams,R.W. and Meyerowitz,E.M. (1997) The CLAVATA1 gene encodes a putative receptor kinase that controls shoot and floral meristem size in *Arabidopsis*. *Cell*, **89**, 575–585.

Fletcher,J.C., Brand,U., Running,M.P., Simon,R. and Meyerowitz,E.M. (1999) Signaling of cell fate decisions by CLAVATA3 in *Arabidopsis* shoot meristems. *Science*, **283**, 1911–1914.

Gonzalez,R.C. and Woods,R.E. (2002) *Digital Image Processing*. Addison-Wesley, Reading, MA.

Jaeger,J., Surkova,S., Blagov,M., Janssens,H., Kosman,D., Kozlov,K.N., Manu, Myasnikova,E., Vanario-Alonso,C.E., Samsonova,M., Sharp,D.H. and Reinitz,J. (2004) Dynamic control of positional information in the early *Drosophila* embryo. *Nature*, **430**, 368–371.

Jönsson,H. and Levchenko,A. (2005) An explicit spatial model of yeast microcolony growth. *Multiscale Model. Simul.*, **3**, 346–361.

Jönsson,H., Shapiro,B.E., Meyerowitz,E.M. and Mjolsness,E. (2003) Signalling in multicellular models of plant development. In Kumar,S. and Bentley,P. (eds), *On Growth, Form and Computers*. Academic Press, London, pp. 156–161.

Jönsson,H., Shapiro,B.E., Meyerowitz,E.M. and Mjolsness,E. (2004) Modeling plant development with gene regulation networks including signaling and cell division. In Kolchanov,N. and Hofestaedt,R. (eds), *Bioinformatics of Genome Regulation and Structure*. Kluwer Academic Publishers, Boston, MA.

Lenhard,M. and Laux,T. (2003) Stem cell homeostasis in the *Arabidopsis* shoot meristem is regulated by intercellular movement of CLAVATA3 and its sequestration by CLAVATA1. *Development*, **130**, 3163–3173.

Mayer,K.F., Schoof,H., Haecker,A., Lenhard,M., Jurgens,G. and Laux,T. (1998) Role of WUSCHEL in regulating stem cell fate in the *Arabidopsis* shoot meristem. *Cell*, **95**, 805–815.

Meinhardt,H. (1982) *Models of Biological Pattern Formation*. Academic Press, London.

Meyerowitz,E.M. (1997) Genetic control in cell division patterns in developing Plants. *Cell*, **88**, 299–308.

Mjolsness,E. (2001) Trainable gene regulation networks with application to *Drosophila* pattern formation. In Bower,J.M. and Bolouri,H. (eds), *Computational Modeling of Genetic and Biochemical Networks*. MIT Press, Cambridge, MA.

Mjolsness,E., Sharp,D.H. and Reinitz,J. (1991) A connectionist model of development. *J. Theor. Biol.*, **152**, 429–454.

Press,W.H., Teukolsky,S.A., Vetterling,W.T. and Flannery,B.P. (1992) *Numerical Recipes in C. The Art of Scientific Computing*. Cambridge University Press, NY.

Prigogine,I. and Lefever,R. (1968) Symmetry breaking instabilities in dissaptive systems. *J. Chem. Phys.*, **48**, 1695–1700.

Prusinkiewicz,P. (2004) Modeling plant growth and development. *Curr. Opin. Plant Biol.*, **7**, 79–83.

Reddy,V.G., Heisler,M.G., Ehrhardt,D.W. and Meyerowitz,E.M. (2004) Real-time lineage analysis reveals oriented cell divisions associated with morphogenesis at the shoot apex of *Arabidopsis thaliana*. *Development*, **131**, 4225–4237.

Reinhardt,D., Frenz,M., Mandel,T. and Kuhlemeier,C. (2003) Microsurgical and laser ablation analysis of interactions between the zones and layers of the tomato shoot apical meristem. *Development*, **130**, 4073–4083.

Sharma,V.K., Carles,C. and Fletcher,J.C. (2003) Maintenance of stem cell populations in plants. *Proc. Natl Acad. Sci. USA*, **30**, 11823–11829.

Schoof,H., Lenhard,M., Haecker,A., Mayer,K.F., Jurgens,G. and Laux,T. (2000) The stem cell population of *Arabidopsis* shoot meristems in maintained by a regulatory loop between the CLAVATA and WUSCHEL genes. *Cell*, **100**, 635–644.

Steeves,T.A. and Sussex,I.M. (1998) *Patterns in Plant Development*. Cambridge University Press, NY.

Turing,A.M. (1952) The chemical basis for morphogenesis. *Philos. Trans. R. Soc. Lond., B*, **237**, 37–72.

von Dassow,G., Meir,E., Munro,E.M. and Odell,G.M. (2000) The segment polarity network is a robust developmental module. *Nature*, **406**, 188–192.

Weigel,D. and Jurgens,G. (2002) Stem cells that make stems. *Nature*, **415**, 751–754.

Xu,C. and Prince,J.L. (1998) Snakes, shapes, and gradient vector flow. *IEEE Trans. Image Process.*, **7**, 359–369.